Desalination and Water Treatment
www.deswater.com

doi: 10.1080/19443994.2015.1042057

57 (2016) 11133–11142
May

Taylor & Francis
Taylor & Francis Group

Fast and selective determination of ammonia in aqueous solutions using immobilized iron(III) oxide nanoparticles on the agarose membrane

Kiomars Zargoosh[a,*], Fatemeh Farhadian Babadi[a], Mohammad Hosseini[b], Ali Hossein Kianfar[a]

[a]*Department of Chemistry, Isfahan University of Technology, Isfahan 84156-83111, Iran, Tel. +98 3133913287; emails: Kiomarszargoosh@cc.iut.ac.ir (K. Zargoosh), fatemefarhadiyan@yahoo.com (F. Farhadian Babadi), Tel. +98 3133913245; email: akianfar@cc.iut.ac.ir (A.H. Kianfar)*

[b]*Department of Chemistry, Islamic Azad University of Arak, Arak, Iran, Tel. +98 6632224126; email: smhosseini2007@gmail.com*

Received 4 July 2014; Accepted 12 April 2015

ABSTRACT

A highly selective and low-cost optical membrane for sensing aqueous ammonia (NH_3) based on the simultaneous production and immobilization of Fe_2O_3 nanoparticles onto agarose membrane was prepared. Iron oxide nanoparticles were synthesized via mild decomposition of iron(III) complex with Schiff base ligand N,N′-disalicylidenetrimethylenediamine (Salpn) in aqueous solutions at 45°C. The proposed method has no problems about fuel consumption and environmental pollution by toxic solvents. The phase, size, and morphology of the prepared iron oxide nanoparticles were characterized by scanning electron microscopy, atomic force microscopy, IR spectroscopy, and X-ray diffraction analysis. The proposed sensor displays a calibration response for ammonia over a concentration range of 1.3×10^{-7}–4.2×10^{-5} mol l^{-1} with a limit of detection of 3.1×10^{-8} mol l^{-1} and a response time of less than 3 min. In addition to its high stability, reproducibility, and relatively long lifetime, the proposed optical sensor revealed good selectivity for ammonia over potential interfering species.

Keywords: Ammonia; Agarose; Iron(III) oxide; Nanoparticle; Optical sensor; Fe_2O_3

1. Introduction

Ammonia (NH_3) is an essential molecule for natural synthesis of biomolecules such as proteins, nucleic acids, and enzymes. In addition, it has wide applications in agricultural and industrial sectors for production of fertilizers, pharmaceuticals, surfactants, colorants, urea, and nitric acid.

On the other hand, ammonia is toxic, and thus the excess presence of ammonia in the atmosphere and environment and drinking waters may create potential hazards to human being and ecosystems. The maximum safe level of ammonia is 25 ppm for long-term exposure (8 h) and 35 ppm for short-term exposure (15 min) [1]. Due to the toxic nature of ammonia, many different detection systems such as metal oxide gas sensors [2], IR adsorption-based assays [3], optical fiber sensors [4], and electrochemical methods [5] have been developed for ammonia concentration measurements.

However, there are two main limitations about applicability of the commonly used ammonia detection systems. First, large number of the commercially

*Corresponding author.

available sensors can only be used for gaseous ammonia and there are only very few sensors which are able to determine the ammonia content of the aqueous samples [6,7]. It should be noted that ammonia has adverse effect on oxygen balance in the aquatic environment, thus discharges of wastewaters containing NH_3 are subject to legislative control and precise determination of NH_3 in drinking water, environmental samples, and industrial wastes is the goal of several researches [8].

Secondly, it is well established by now that SnO_2-based gas sensors (as commonly used ammonia sensors) operate on the principle of conductance change due to chemisorption of gas molecules to the sensing layer. As can be concluded from this model, metal oxide sensors are not selective to one particular gas and serious cross-sensitivity of them toward atmospheric gasses such as nitrogen, oxygen, carbon dioxide, and water vapor has been reported in the literature [9,10].

Electrochemical sensors can be used for determination of aqueous ammonia, but in most cases, there is no data on their selectivity toward possible interfering species. For example, Abaker et al. [11] reported an electrochemical sensor based on immobilization of the α-Fe_2O_3 nanoellipsoids on the glassy carbon electrode (GCE) for determination of aqueous ammonia, but without selectivity investigation. Modified GCE with ZnO nanopencils has been used by Dar et al. [12] for determination of ammonia in aqueous solution, but without any data on the selectivity issue. Electrodes based on the polyurethane–clay nanohybrids have been proposed by Khan et al. [13] for determination of aqueous ammonia, again without selectivity consideration.

To overcome these problems, optical sensor seems to be a suitable choice because its response mechanism is based on the especial interaction (such as covalent bonding, hydrogen bonding, and complex formation) between ammonia and sensing component of the sensor; thus, optical sensors are the most selective ammonia sensors in gas phase. In addition, by appropriate immobilization of the sensor components onto proper supports, optical sensors can be used for determination of ammonia in aqueous samples. Due to these reasons, optical sensors received considerable attention in recent years and several modifications have been made on their performance characteristics. It seems that outstanding improvements in the performance characteristics of the ammonia optical sensors have been achieved using microspheres and nanoparticles. Ling et al. [7] developed a reflectometric NH_3 sensor based on a single-step immobilization of Co^{2+} ion onto high-capacity Dowex HCR-W2 microspheres that was suitable for direct determination of NH_3 in highly colored water samples. Pandey et al. [6] fabricated a more complicated sensor using biopolymer/silver nanoparticles nanocomposite and surface plasmon resonance detection system for determination of ammonia in biological fluids. Recently, Tavoli and Alizadeh [14] constructed an ammonia gas sensor by doping the eriochrome cyanine R in nanostructured polypyrrole film.

However, in many cases, construction of nanoparticle-based optical sensors needs expensive metal/metal oxide nanoparticles and high-cost detection systems [15]. In addition, there are several limitations about the immobilization of the obtained nanoparticles on the supports, especially with biocompatible supports. For example, most of the nanoparticle production methods include heating steps at temperatures above 250˚C, thus require special apparatus and obviously cannot be used for immobilization of the obtained nanoparticles on the heat-sensitive supports. Consuming of large amounts of fuel and toxic organic reagents such as ethylene glycol and octyl amine are other drawbacks of these methods. These problems seriously limited the applicability of nanoparticle-based optical sensors for routine analysis of environmental samples.

In this work, we propose a novel optical membrane for determination of aqueous ammonia based on the simultaneous production and immobilization of the iron(III) oxide, Fe_2O_3, nanoparticles onto transparent agarose membrane. The iron oxide nanoparticles were synthesized via mild decomposition of iron(III) complex with Schiff base ligand N,N´-disalicylidenetrimethylenediamine (Salpn) in aqueous solutions at 45˚C. The Fe_2O_3 nanoparticles were simply immobilized onto the transparent agarose membrane by immersing a previously activated agarose membrane in the reaction beaker for 4 h under stirring. The reduction in the optical absorption of this reddish-brown Fe_2O_3 nanoparticle–agarose membrane in the presence of aqueous ammonia was recorded by UV–vis spectrophotometer and used as an analytical signal. It should be noted that this strategy can be used for the preparation of other metal oxide nanoparticles under mild conditions and in water instead of toxic solvents. Additionally, both iron(III) salts and agarose are low-cost materials, thus the constructed ammonia sensor is very simple and cheap.

2. Experimental

2.1. Reagents

Previously reported method was used for synthesis of the Schiff base ligand N,N´-disalicylidenetrimethylenediamine, H_2Salpn, via condensation

reaction between 1,3-propanediamine and 2-hydroxybenzaldehyde [16] (see Fig. 1). Ethanol, epichlorohydrine, sodium hydroxide, and hydrochloric acid were purchased from Merck (Darmstadt, Germany). The metal salts of all cations used (all from Merck) were of the highest purity available and used without any further purification. Ammonia solutions were prepared from a stock ammonia solution (from Aldrich) by proper dilution methods using double-distilled water.

Fe^{3+} stock solution (1.5×10^{-3} M) was prepared by dissolving appropriate amounts of $Fe(Cl)_3{\cdot}6H_2O$ in water and diluted to 50 ml in a standard flask. Sample solutions were prepared by appropriate dilution. The pH values of the test samples were adjusted using 0.1 M HCl or NaOH solution. Double-distilled water was used throughout.

Salpn stock solution (5.0×10^{-4} M) was prepared by dissolving appropriate amounts of it in ethanol and diluted to 50 ml in a standard flask. Sample solutions were prepared by appropriate dilution.

2.2. Apparatus

Absorption measurements were carried out on a Hitachi U-2000 spectrophotometer. A Jenway (USA) model 3020 pH meter with a combined glass electrode was used after calibration against standard Merck buffers for pH determinations. A homemade polyacrylamide holder was used for holding agarose membranes inside the quartz cells of the spectrophotometer. A totally glass Fisons (UK) double distiller was used for the preparation of doubly distilled water. Shaking Bath model OLS200 from Grant Instruments was used for shaking the agarose membrane during epichlorohydrine activation. Field-emission scanning electron microscopy (FE-SEM) S-4160 Hitachi (Japan) and atomic force microscopy (AFM) Nanos Bruker (Germany) were used to investigate the morphology of the Fe_2O_3–agarose membrane and size distribution of the immobilized Fe_2O_3 particles. Fourier transform infrared (FT-IR) spectra were obtained with a Bruker model Equinox 55 LS101 FT-IR spectrophotometer. X-ray diffraction (XRD) measurements were carried out to study the crystalline phase of Fe_2O_3 using a Siemens D-5000 X-ray diffractometer (Germany) with Cu–Ka radiation.

3. Results and discussion

3.1. Synthesis of Fe(Salpn) complex

As is clear from Fig. 1, Salpn and its derivatives are tetradentate ligands and can adopt different conformations and bind in a number of coordination modes, according to the geometric requirements of the metal ions and metal: ligand concentration ratio, thus the complexes of type Fe(Salpn) and $Fe(Salpn)_2$ have been reported in the literature [17]. In this work, the Fe(Salpn) complex was simply synthesized by mixing appropriate volumes of the Fe^{3+}(5.0×10^{-4} M) and Salpn (5.0×10^{-4} M) solutions at room temperature (see Fig. 2). The blue complex was immediately formed and the mole ratio study reveals that metal: ligand ratio is 1:1.

3.2. Preparation and epoxy activation of the agarose membrane

For the preparation of transparent agarose membranes, a method described elsewhere [18] was used with some modifications. A weighed amount, 0.4 g, of agarose powder was mixed with 20 ml doubly distilled water. To obtain a viscose solution, the mixture was stirred at 90°C until its volume decreased to 15 ml. In most cases, removing the bubbles from viscose solutions is a tedious and time-consuming work. Fortunately, we found that by immersion of the beaker containing viscose agarose solution in an ultrasonic bath for 3 min, the bubbles can be removed completely. The final transparent, viscose solution was dispersed between two 20 cm × 20 cm dust-free glass plates, applying a gentle pressure. Borders of one of the glass plates were already lined with a 0.25 mm thickness tape to adjust the thickness of the

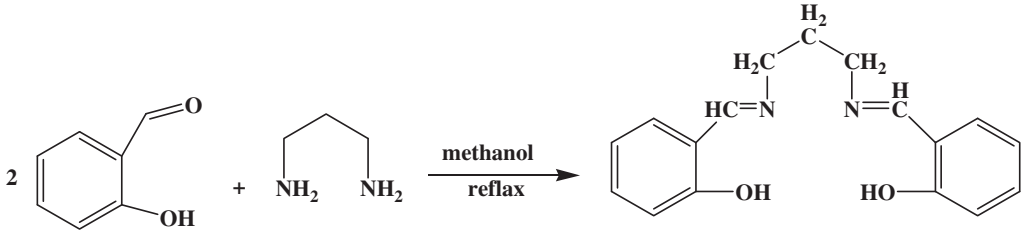

Fig. 1. Synthesis of Salpn via condensation reaction.

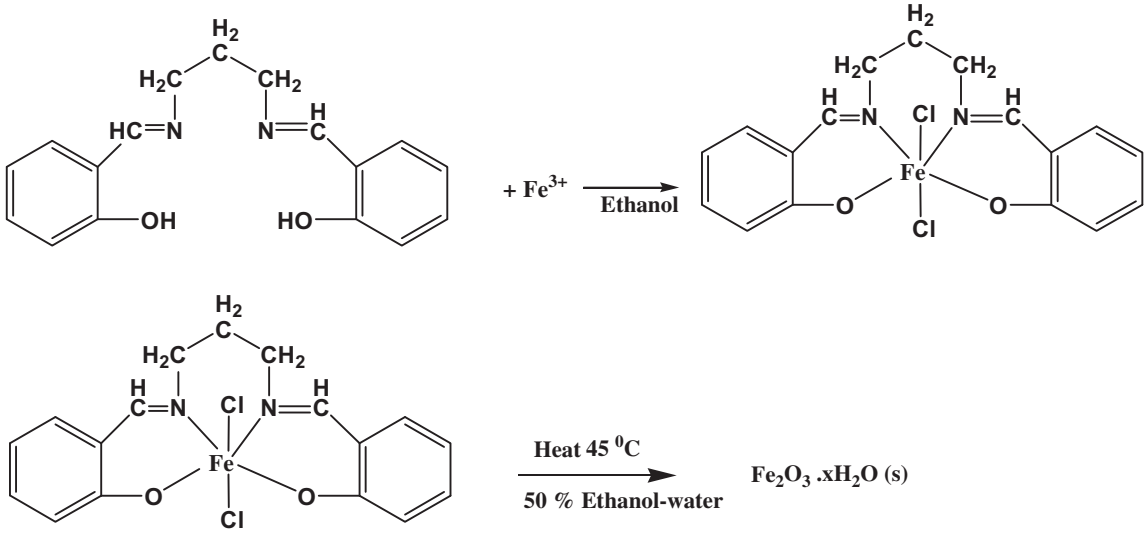

Fig. 2. Synthesis of Fe(Salpn) complex and production of Fe_2O_3 nanoparticles via decomposition of Fe(Salpn) complex.

membrane. After cooling, the solidified membrane was cut into appropriate pieces and stored at 4°C under 50% ethanol solution. For the epoxy activation, an epichlorohydrine method was used [19]. Briefly, agarose membranes were immersed in 10 ml of a solution containing epichlorohydrine (7% (V/V)) and NaOH (0.6 M). Then, the mixture was shaken at 45°C in a shaker bath for 2 h. Finally, the activated agarose membranes were washed with 500 ml of distilled water.

3.3. Preparation of Fe_2O_3 nanoparticles and immobilization of them on agarose membrane

In primary experiments, it was found that Fe (Salpn) complex is heat sensitive and can be decomposed in aqueous solution even with mild heating. In each experiment, 100 ml of the 5.0×10^{-4} mol l^{-1} aqueous solution of the Fe(Salpn) complex was heated at 45°C to decompose slowly and produce $Fe_2O_3.xH_2O$ nanoparticles. The reddish-brown color precipitate was separated from the aqueous solution and dried at 110°C for 12 h. Fig. 3 shows the SEM image of the obtained powder. As is clear from the SEM image, the diameters of the Fe_2O_3 nanoparticles are about 45 nm and Fe_2O_3 nanoparticles have homogeneous size.

The prepared $Fe_2O_3.xH_2O$ was dried at 110°C for 12 h and its XRD pattern was recorded using a Siemens D-5000 X-ray diffractometer. The XRD pattern of the dried sample is shown in Fig. 4. The peak analysis indicates that the prepared iron oxide is present in a well-crystalline rhombohedral hematite (α-Fe_2O_3) phase. The reflection peak positions and relative

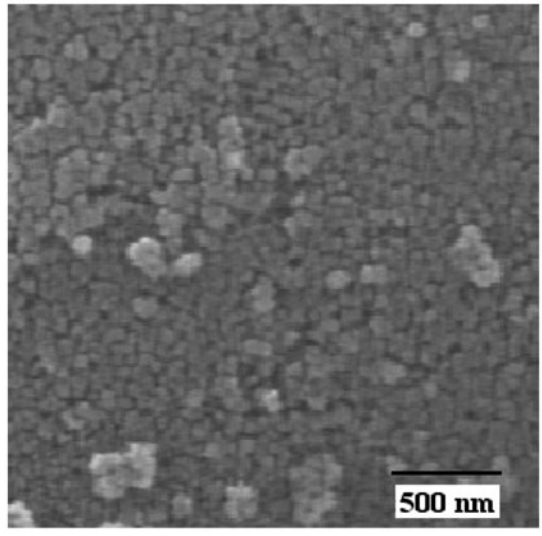

Fig. 3. SEM image of the obtained Fe_2O_3 nanoparticles.

intensities of the prepared Fe_2O_3 agree well with XRD patterns for hematite (α-Fe_2O_3) in the literature [20, http://claymin.geoscienceworld.org/content/45/1/1/F1.expansion.html]. No reflections for other impurities such as FeOOH and Fe3O4 are found in the pattern which further confirms that the synthesized Fe_2O_3 nanoparticles are pure.

The FT-IR spectra were obtained by the KBr pellet technique with about 8 wt% of the Fe_2O_3 sample. The broad peaks at 453 and 632 cm^{-1} clearly show that the obtained precipitate is Fe_2O_3. In aqueous solutions and under neutral pH conditions, the most expected

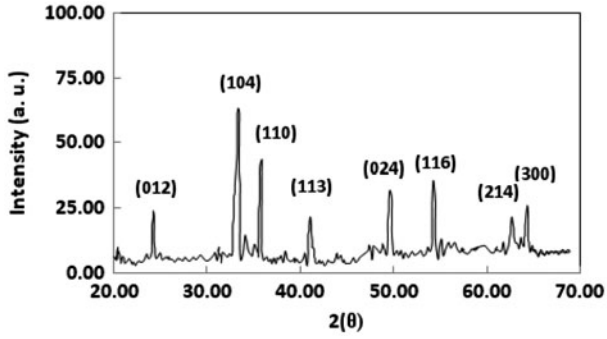

Fig. 4. XRD pattern of the obtained Fe_2O_3 nanoparticles.

reaction of the Fe^{3+} ions is precipitation via formation of $Fe(OH)_3$, $Fe_2O_3.xH_2O$, particles. But in the presence of epoxy-activated agarose membrane, some of these *in situ*-produced $Fe(OH)_3$ small particles can directly interact with hydroxyl groups of the activated membrane surface and be immobilized on it. This primary immobilization of the $Fe_2O_3.xH_2O$ on the activated membrane may involve hydrogen bonding or dipole–dipole interactions. Formation of the oxygen–oxygen or metal–oxygen bonds between $Fe_2O_3.xH_2O$ particles and agarose surface may be the next step to produce firmly immobilized $Fe_2O_3.xH_2O$ on the agarose membrane.

To study the stability of the immobilized nanoparticles on the membranes, the agarose membranes were immersed in reaction beaker containing 1.0×10^{-4} mol l^{-1} aqueous solution of the Fe(Salpn) complex for 2 h under shaking. The resulting reddish-brown color membranes were thoroughly washed with water on a glass filter, soaked in water overnight, and washed again with a large volume of water to displace any non-bound iron(III) oxide. The immobilized iron(III) oxide was completely stable and could not be removed by multiple washing with water or ethanol, thus formation of the covalent bond between the agarose surface and iron(III) oxide particles is a possible mechanism for immobilization of them on the agarose membranes. Fig. 5 shows the immobilized iron(III) oxide on the agarose membrane together with its UV–vis spectra. As is clear from Fig. 5, the reddish-brown appearance of the prepared membrane confirms that the immobilized layer must be $Fe_2O_3.xH_2O$.

Fig. 6 shows the SEM images of the agarose membranes before and after immobilization of Fe_2O_3 nanoparticles on them. As is clear from SEM images, the Fe_2O_3 nanoparticles can be uniformly immobilized on the agarose membranes. An AFM image of the immobilized Fe_2O_3 nanoparticles on the agarose membranes together with size distribution curves have been depicted in Fig. 7. As is clear from Fig. 7, the diameters of the Fe_2O_3 nanoparticles are about 45 nm and Fe_2O_3 nanoparticles include homogeneous particles. It must be noted that immobilization of the metal oxides on suitable supports is of great importance because most valuable metal oxide catalyst must be immobilized on suitable supports. The proposed method opens a novel route for production and immobilization of nanoparticles of the metal oxides, which their cations can form heat-sensitive complexes with Schiff base ligands. In addition, recording the absorption spectra of the metal oxides in the solid state needs complicated apparatus. Immobilization of the metal oxides on the transparent agarose membranes offers a simple and low-cost method for direct recording of their absorption spectra.

3.4. Optimization of the conditions for the preparation of Fe_2O_3–agarose membrane

In order to obtain an appropriate Fe_2O_3 loading on the agarose membrane, the experimental conditions must be optimized. To study the effects of the pH of the Fe(Salpn) solution on the Fe_2O_3 loading, activated agarose membranes were shaken in 1.0×10^{-4} M solutions of Fe(Salpn) at 45°C for 2 h. The results were depicted in Fig. 8. As can be seen from Fig. 8, the maximum immobilization of the Fe_2O_3 is achieved in pH of about 11. This observation is in agreement with these facts that OH^- ions can speed up the decomposition reaction of the Fe(Salpn) complex, and hence, enhance the effective interaction between iron-containing species and membrane surface (via formation of deprotonated hydroxyl group on the agarose surface) and facilitate the precipitation of the $Fe_2O_3.xH_2O$ particles. At pH values lower than 7, the Fe(Salpn) is decomposed slowly, and hence, longer time was needed to obtain acceptable loading of Fe_2O_3 nanoparticles on the agarose membranes. Therefore, pH of 11 was selected as the optimum pH for immobilization of Fe_2O_3 on the activated agarose membranes.

To study the effects of the Fe(Salpn) concentration on the Fe_2O_3 loading, the temperature of the Fe(Salpn) solution was fixed at 45°C and the pH of the solution was kept at 11. Investigation of the effect of Fe(Salpn) concentration on the Fe_2O_3 immobilization on the membrane indicated a continuous increase in the membrane absorbance by increasing the Fe(Salpn) concentration from 3×10^{-7} to 1×10^{-2} M. High loadings, however, could unacceptably decrease the transmittance of the membrane. Therefore, a Fe(Salpn) concentration of 1×10^{-4} M, resulting in a maximum absorbance of about 0.8, was used as the optimum concentration for immobilization of Fe_2O_3.

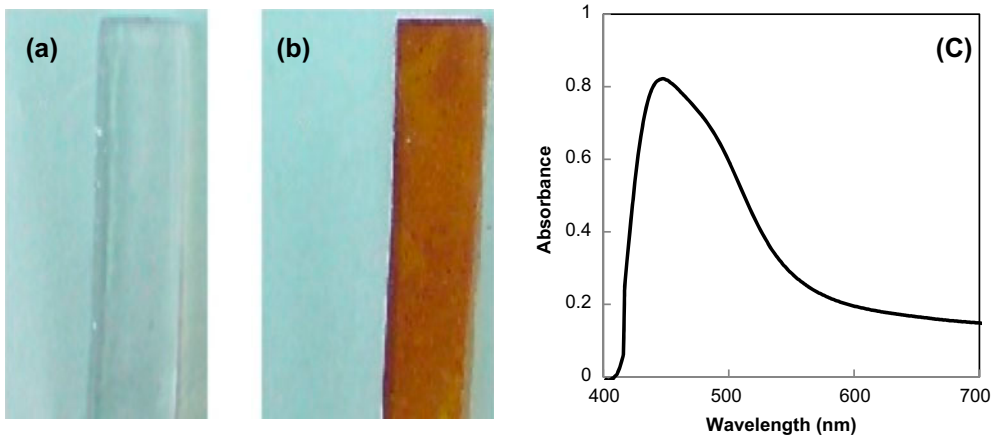

Fig. 5. (a) Agarose membrane, (b) agarose membrane with immobilized Fe_2O_3 nanoparticles, and (c) the UV–vis absorbance of the immobilized Fe_2O_3 nanoparticles on agarose membrane.

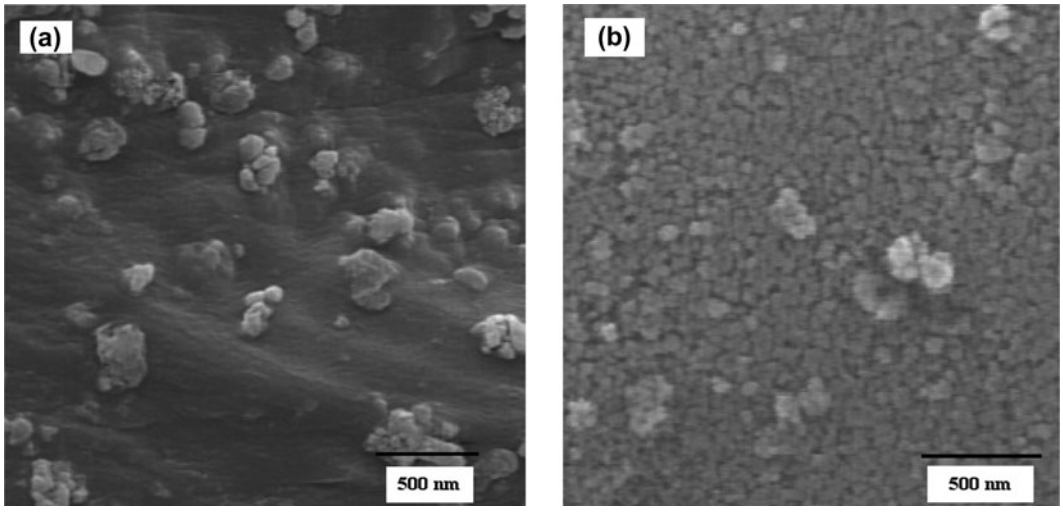

Fig. 6. (a) SEM images of the agarose membrane, agarose membrane without Fe_2O_3 nanoparticles and (b) agarose membrane with immobilized Fe_2O_3 nanoparticles.

Temperature of the Fe(Salpn) solution was the last parameter that was optimized for immobilization of the synthesized nanoparticles. The activated agarose membranes were shaken in 1.0×10^{-4} M solutions of Fe(Salpn) for 2 h. The pH of the Fe(Salpn) solution was kept at 11 and the temperature of the solutions was changed in a range of 10–70˚C. The extent of the Fe_2O_3 loading found to increase with increase in the temperature of Fe(Salpn) solution up to 50˚C. However, at higher temperatures, some degradation in agarose membranes was observed. Thus, to obtain maximum loading of Fe_2O_3 without destructive effects on the agarose membranes, temperature of 45˚C was selected as optimum.

3.5. Measurement procedure and principle of operation

It was found that aqueous ammonia solution can significantly reduce the absorbance of the iron(III) oxide-activated agarose membrane. For production of iron(III) oxide-loaded membranes, epichlorohydrine-activated agarose membranes were shaken in 1.0×10^{-4} M solution of Fe(Salpn) for 2 h at 45˚C and constant pH of 11. Absorbance spectra of the obtained optical membranes in the presence of the varying concentrations of ammonia have been depicted in Fig. 9. The ammonia concentrations are from 1.3×10^{-7} mol l^{-1} (top) to 4.2×10^{-5} mol l^{-1} (bottom) in an aqueous solution of pH 8.0. This reduction in the

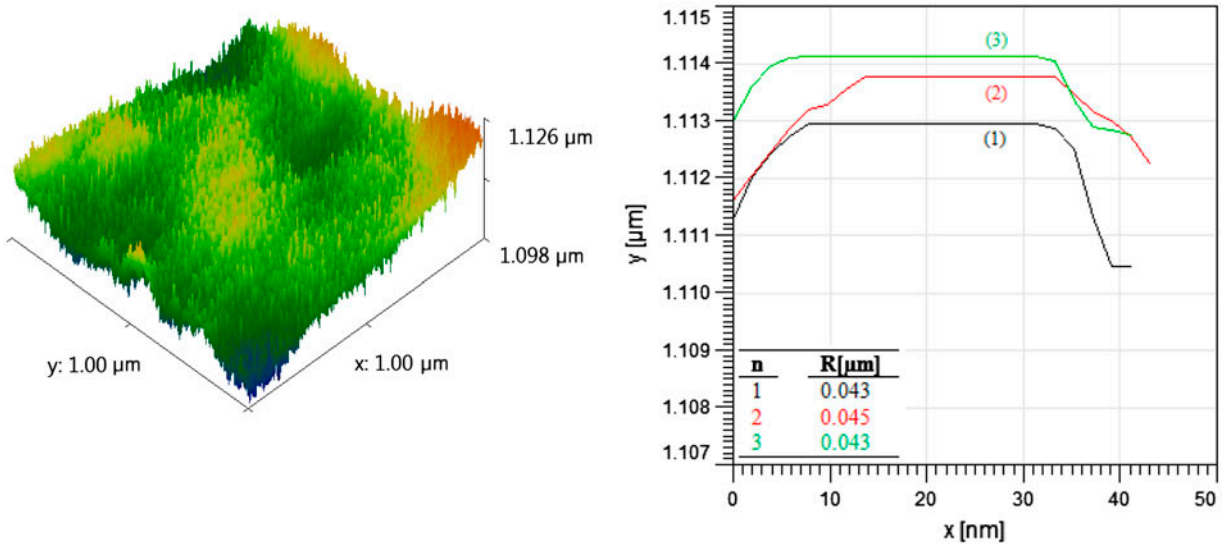

Fig. 7. AFM image of the Fe_2O_3 nanoparicles on the agarose membrane together with size distribution curves.

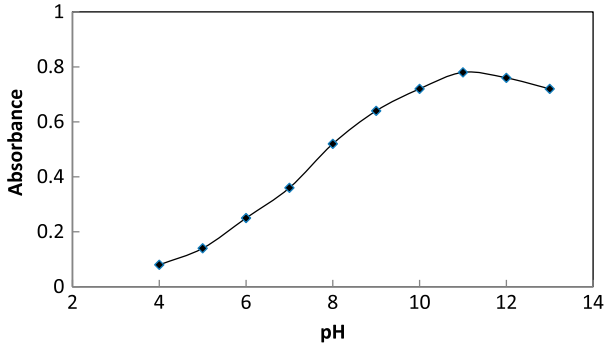

Fig. 8. Effects of pH on the loading of Fe_2O_3 on the agarose membrane.

absorbance may be due to the formation of the non-absorbing complex between ammonia and iron-containing species on the agarose membrane or removing the iron(III) oxide from the membrane surface. It was found that complex formation is responsible for this reduction in the absorbance because the absorbance signal of the proposed optical membrane was recovered completely when the solution was switched from high to low ammonia concentrations. In addition, over the wide range of ammonia concentrations (1.0×10^{-7}–1.0×10^{-3} M) tested, the optical sensor response reaches its equilibrium value in less than 3 min, whereas removing of the iron-containing species from the membrane is basically a non-equilibrium process. In this work, the reduction in the optical absorption of the $Fe_2O_3.xH_2O$-loaded agarose membrane in the

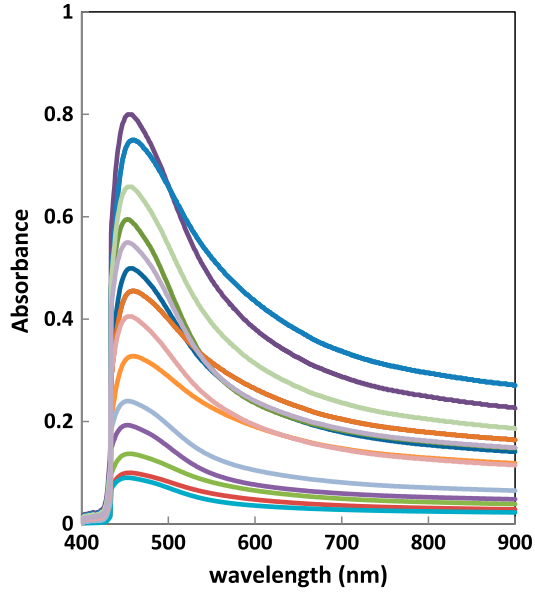

Fig. 9. Absorbance spectra of the proposed optical membrane in the presence of varying concentrations of ammonia. Notes: The ammonia concentrations are from 1.3×10^{-7} mol l^{-1} (top) to 4.2×10^{-5} mol l^{-1} (bottom) in an aqueous solution of pH 8.0.

presence of aqueous ammonia solution at 458 nm was used as an analytical signal.

In all measurements, a 1 cm × 4 cm piece of the prepared agarose optical membrane was mounted in a polyacrylamide holder and placed inside the quartz cell of the spectrophotometer. The absorbance

readings were carried out against a blank cell containing a non-activated agarose membrane. For the study of the effects of different parameters on the response of the optical membrane, absorbance measurements at 458 nm were carried out in an aqueous medium. The absorbance readings for the samples were subtracted from the absorbance of a buffer solution at the same wavelength. The ammonia concentration was then derived using an ordinary calibration curve method.

3.6. Effect of pH of test solution

Fig. 10 shows the influence of pH of test solution on the absorbance response of the proposed ammonia optical sensor. The absorbance measurements were made in the presence of a 1.5×10^{-6} mol l^{-1} ammonia solution of different pH values. The pH of the solutions was adjusted by either HCl or NaOH. It looked more appropriate to use ΔA (the absorbance differences before and after addition of ammonia) rather than absolute A, in this study. As seen, the response of the sensor passes through a more or less plateau between pH 7.8 and 8.5. While, beyond this pH range, the optical response decreased. The diminished signals at pH < 7.8 could be due to the protonation of ammonia that significantly decreases its ligating ability. On the other hand, the reduced absorbance of the sensor at pH > 8.5 is most possibly because of the formation of gaseous ammonia. Thus, in the subsequent experiments, solutions of pH 8.0 adjusted by either HCl or NaOH were used.

3.7. Reproducibility, short-term stability, and lifetime

Efficient regeneration of an optical membrane in a reasonable time is a requirement of its usefulness in multiple usages. The absorbance signal of the proposed optical membrane was recovered when the solution was switched from high to low ammonia concentrations, thus each membrane can be used for replicate determination of ammonia. In addition, due to low cost of the prepared membrane, its application for environmental analysis is economically acceptable.

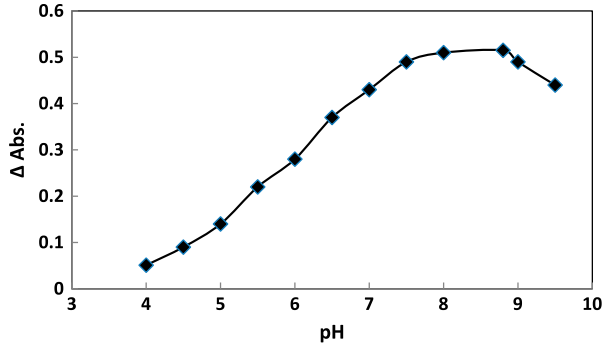

Fig. 10. Effect of pH of the test solution on the response of the proposed optical membrane in the presence of 1.5×10^{-6} mol l^{-1} ammonia.

The reproducibility was examined by preparing eight different membranes under optimum conditions and measuring the absorbance of each membrane in a 1.5×10^{-6} mol l^{-1} ammonia solution (three repeated determinations) at pH 8.0. The resulting coefficient of variation was found to be ±3.3%.

The short-term stability of the optical membrane was studied by its absorbance measurements in contact with a 1.5×10^{-6} mol l^{-1} ammonia solution at pH 8.0 over a period of 6 h. From the absorbance measurements, after every 30 min ($n = 12$), it was found that the response is almost complete with only 4.1% deviation in response after 6 h monitoring. In addition, it was found that the membrane sensor could be stored at 4°C under 50% ethanol solution without any measurable changes in its absorbance for at least 3 weeks, which again implies that the immobilization of iron(III) oxide on the agarose membrane involves covalent bond formation.

3.8. Selectivity

For the selectivity investigation, the interference of different potential interfering species on the response of the proposed optical sensor was examined using a 1.5×10^{-6} mol l^{-1} ammonia solution and variable concentrations of the interfering species at pH 8.0. The tolerance ratio (TR was defined as the ratio of the concentration of interfering species over the concentration of ammonia that caused a relative error of 5%. The resulting tolerance ratios of TR = [interfering species]/[ammonia] are summarized in Table 1. As is obvious from Table 1, the ammonia content of solutions can be selectively determined using the proposed optical sensor in the presence of excess amounts of the potential interferences examined.

The above results indicated that the proposed ammonia optical membrane can be applied to determine traces of ammonia in real samples, in the presence of excess of several other coexisting species. Such high level of selectivity is critical for the determination of ammonia in complex matrixes such as environmental waters, where the interference from other coexisting species limits the application of the commercial optical methods [21].

Table 1
TR for different potential interfering species in the determination of 1.5×10^{-6} mol l^{-1} ammonia

Interfering species	Tolerance ratio (TR)
Pyridine	368
Butylamine	321
Propylamine	273
Ethylamine	120
Methylamine	125
Ethanol	1,000<
Acetone	1,000<
Acetonitrile	1,000<
Methanol	286

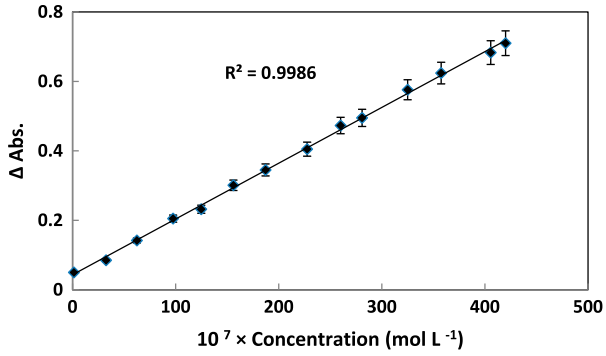

Fig. 11. Calibration plot of ΔAbs against [ammonia] for the proposed optical membrane.

3.9. Calibration curve and dynamic response time

As mentioned in previous sections, Fe_2O_3–agarose membrane has reddish-brown appearance with maximum absorption about 458 nm. The UV–vis spectra of the proposed optical membrane at pH 8.0 and in the presence of increasing concentration of ammonia are shown in Fig. 9. As is obvious, upon effective interaction between ammonia and immobilized Fe_2O_3 particles, the membrane color turns from reddish-brown to colorless; the absorbance (at λ_{max} = 458 nm) decreases with increase in concentration of ammonia in aqueous solution. The response curve was linear in an ammonia concentration range of 1.3×10^{-7}–4.2×10^{-5} mol l^{-1}. A line was fitted to the experimental points and the following equation was achieved for the calibration curve shown in Fig. 11, with an R^2 value of 0.9986:

$$\Delta Abs = 16060\,[\text{ammonia}] + 0.0434 \quad (1)$$

in which Abs stands for absorbance. The detection limit based on 3δ of the blank was calculated to be 3.1×10^{-8} mol l^{-1} ammonia.

The dynamic response time of the proposed optical membrane was studied by plotting ΔA as a function of time upon step changing of the ammonia concentration in solution, over a concentration range of 1.3×10^{-7}–4.2×10^{-5} mol l^{-1}. It was found that, over the entire concentration range of ammonia tested, the optical membrane response reaches its equilibrium value in less than 3 min.

Table 2
Results of three replicate determinations of ammonia in different samples

	Amount of ammonia (mol l^{-1})	
Sample	Added	Found by sensor
Spiked tap water (1)	8.0×10^{-7}	$8.07(\pm0.05) \times 10^{-7}$
Spiked tap water (2)	1.0×10^{-6}	$1.03(\pm0.03) \times 10^{-6}$
Spiked tap water (3)	5.0×10^{-6}	$4.87(\pm0.10) \times 10^{-6}$
Spiked tap water (4)	1.0×10^{-5}	$1.02(\pm0.06) \times 10^{-5}$

3.10. Analytical applications

The proposed ammonia optical sensor was found to work well under laboratory conditions. It was successfully applied to the direct determination of ammonia content of the spiked tap water samples (Table 2).

Table 3
General performance characteristics of recently reported aqueous ammonia optical sensors

Active reagent	Linear range (mol l^{-1})	Detection limit (mol l^{-1})	Response time
Silver nanoparticle nanocomposite [6]	5.9×10^{-5}–2.9×10^{-3}	5.9×10^{-5}	2–3 s
Co^{2+} ions [7]	6.0×10^{-2}–2.9×10^{-1}	2.0×10^{-2}	6 min
Coumarin derivatives [22]	5.9×10^{-8}–2.9×10^{-4}	5.9×10^{-8}	20 min
Bromophenol blue [23]	6.0×10^{-7}–1.0×10^{-3}	6.0×10^{-7}	10 min
Xanthene [24]	3.0×10^{-7}–6.0×10^{-5}	1.0×10^{-7}	20–30 min
Iron(III) oxide nanoparticle, this work	1.3×10^{-7}–4.2×10^{-5}	3.1×10^{-8}	3 min

From the data, taken from three replicate measurements, it is immediately obvious that there is a satisfactory agreement between spiked amounts and those obtained by the proposed ammonia optical sensor.

4. Conclusion

The results presented in this paper demonstrated that the immobilization of the Fe_2O_3 nanoparticles on the agarose membrane could result in a stable, selective, and sensitive optical sensor for ammonia. A comparison of the performance characteristics of the developed ammonia optical sensor with those of the recently reported ones [6,7,22–24] (Table 3) revealed that the proposed sensor possesses some improvements over the existing optical sensors for ammonia with respect to linear range, limit of detection and, especially, response time. Satisfactory results were obtained from the application of the proposed sensor to the direct determination of ammonia content of the spiked tap water samples.

References

[1] Occupational Exposure Limits 2000 Guidance Note EH40/2000, HSE Books, 2000.
[2] K. Zakrzewska, Mixed oxides as gas sensors, Thin Solid Films 391 (2001) 229–238.
[3] M. Fehér, P.A. Martin, A. Rohrbacher, A.M. Soliva, J.P. Maier, Inexpensive near-infrared diode-laser-based detection system for ammonia, Appl. Optics. 32 (1993) 2028–2030.
[4] H. Manap, R. Muda, S. O'Keeffe, E. Lewis, Ammonia sensing and a cross sensitivity evaluation with atmosphere gases using optical fiber sensor, Procedia Chem. 1 (2009) 959–962.
[5] B.A. López de Mishima, H.T. Mishima, Ammonia sensor based on propylene carbonate, Sens. Actuators, B 131 (2008) 236–240.
[6] S. Pandey, G.K. Goswami, K.K. Nanda, Green synthesis of biopolymer–silver nanoparticle nanocomposite: An optical sensor for ammonia detection, Int. J. Biol. Macromol. 51 (2012) 583–589.
[7] T.L. Ling, M. Ahmad, L.Y. Heng, A novel optical ammonia sensor based on reflectance measurements for highly polluted and coloured water, Sens. Actuators, B 171–172 (2012) 994–1000.
[8] K.N. Andrew, P.J. Worsfold, M. Comber, On-line flow injection monitoring of ammonia in industrial liquid effluents, Anal. Chim. Acta. 314 (1995) 33–43.
[9] B. Timmer, W. Olthuis, A. Berg, Ammonia sensors and their applications—A review, Sens. Actuators, B 107 (2005) 666–677.
[10] Y. Huang, L. Wieck, S. Tao, Development and evaluation of optical fiber NH_3 sensors for application in air quality monitoring, Atmos. Environ. 66 (2013) 1–7.
[11] M. Abaker, A. Umar, S. Baskoutas, G.N. Dar, S.A. Zaidi, S.A. Al-Sayari, A. Al-Hajry, S.H. Kim, S.W. Hwang, A highly sensitive ammonia chemical sensor based on α-Fe_2O_3 nanoellipsoids, J. Phys. D: Appl. Phys. 44 (2011) 425401–425408.
[12] G.N. Dar, A. Umar, S.A. Zaidi, S. Baskoutas, S.W. Hwang, M. Abaker, A. Al-Hajry, S.A. Al-Sayari, Ultra-high sensitive ammonia chemical sensor based on ZnO nanopencils, Talanta 89 (2012) 155–161.
[13] S.B. Khan, M.M. Rahman, E.S. Jang, K. Akhtar, H. Han, Special susceptive aqueous ammonia chemi-sensor: Extended applications of novel UV-curable polyurethane-clay nanohybrid, Talanta 84 (2011) 1005–1010.
[14] F. Tavoli, N. Alizadeh, Optical ammonia gas sensor based on nanostructure dye-doped polypyrrole, Sens. Actuators, B 176 (2013) 761–767.
[15] H.S. Mader, O.S. Wolfbeis, Optical ammonia sensor based on upconverting luminescent nanoparticles, Anal. Chem. 82 (2010) 5002–5004.
[16] K.J. van Bommel, W. Verboom, H. Kooijman, A.L. Spek, D.N. Reinhoudt, Rhenium(V)−salen complexes: Configurational control and ligand exchange, Inorg. Chem. 37 (1998) 4197–4203.
[17] Z. Smékal, F. Březina, Z. Šindelář, R. Klička, Mononuclear and binuclear complexes of iron(III) with the tetradentate Schiff base derived from salicylaldehyde and 1,2 diaminopropane, Polyhedron 15 (1996) 1971–1974.
[18] P. Hashemi, M. Hosseini, K. Zargoosh, K. Alizadeh, High sensitive optode for selective determination of Ni^{2+} based on the covalently immobilized thionine in agarose membrane, Sens. Actuators, B 153 (2011) 24–28.
[19] I. Matsumoto, Y. Mizuno, N. Seno, Activation of sepharose with epichlorohydrine and subsequent immobilization of ligand for affinity adsorbent, J. Biochem. 85 (1979) 1091–1098.
[20] I.V. Chernyshova, M.F. Hochella Jr., A.S. Madden, Size-dependent structural transformations of hematite nanoparticles. 1. Phase transition, Phys. Chem. Chem. Phys. 9 (2007) 1736–1750.
[21] P.L. Searle, The berthelot or indophenol reaction and its use in the analytical chemistry of nitrogen. A review, Analyst 109 (1984) 549–568.
[22] K. Waich, S. Borisov, T. Mayr, I. Klimant, Dual lifetime referenced trace ammonia sensors, Sens. Actuators, B 139 (2009) 132–138.
[23] K.T. Lau, S. Edwards, D. Diamond, Solid-state ammonia sensor based on Berthelot's reaction, Sens. Actuators, B 98 (2004) 12–17.
[24] K. Waich, T. Mayr, I. Klimant, Fluorescence sensors for trace monitoring of dissolved ammonia, Talanta 77 (2008) 66–72.